Pure & Appl. Chem., Vol.55, No.5, pp.833-844, 1983.
Printed in Great Britain.

0033-4545/83/050833-12$03.00
Pergamon Press Ltd.

THE NATURE OF DEFECTS AND THEIR ROLE IN LARGE DEFORMATION AND FRACTURE OF ENGINEERING THERMOPLASTICS

H.H. Kausch

Polymer Laboratory, Swiss Federal Institute of Technology
Lausanne, 32, chemin de Bellerive, CH-1007 Lausanne

Abstract - In this paper molecular defects (chain scission, weak bonds), network irregularities (mostly concerning entanglements), flaws and inclusions and production related defects are discussed with respect to crazing, large deformations and rupture of polymers.

INTRODUCTION

Plastic materials are made up of long chain molecules which are interconnected by chemical crosslinking points (thermosetting resins, vulcanized rubbers), crystalline regions (semi-crystalline thermoplastics), and physical entanglements (practically all polymers). The networks formed in this way are often modified (stabilized, plasticized, filled and/or reinforced). An average commercial plastic material, therefore, is a heterogeneous system. Even if it is perfect, it contains quite different structural elements. Depending on their mode of interaction (slippage or elastic loading), a variety of responses occurs (e.g. viscoelastic deformation, crazing, yielding, brittle or ductile failure). In a previous presentation (1) the molecular mechanisms leading to different failure patterns have been discussed. In this paper prime consideration will be given to material defects on a molecular, microscopic and macroscopic level. In order to elucidate their role, the "normal behavior" of stressed polymers will briefly be introduced in the following section.

STRUCTURAL ELEMENTS AND THEIR RESPONSE TO LOAD

In a defect-free amorphous polymer such as PS, PMMA, or PC one would have to consider as structural elements the chain ends, the statistical chain segments (0.4 to 1 nm in length), the chain sections between entanglement points (2 to 10 nm), and the statistically coiled molecules. Depending on the production technique, a distinct globular superstructure may also be present (as for instance in PVC). In the case of crystalline polymers evidently the presence of lamellar crystalline regions and of spherulites has to be taken into account.

The normal response of a thermoplastic material to increasing loads will be an **anelastic widening** of the "lattice", bond rotation in the main chain leading to a change of conformation and **creep,** segment rotation and **craze initiation** (where appropriate), and a brittle **(fracture)** or ductile instability (segment slip and **yielding** followed by large scale chain orientation and either **strain hardening** or **flow).** In the presence of a superstructure these phenomena will preferentially develop at the intergranular or interspherulitic boundaries.

An apparent paradox should be noted. Whereas it has become quite clear that **chain scission** plays no significant role in the deformation and fracture of **isotropic** polymers (2), **chain length** is a quite important parameter. This is well demonstrated by a plot of fracture surface energy G_{Ic} vs molecular weight (Fig. 1).

Short chains with a molecular weight smaller than the entanglement molecular weight M_c are easily - and practically individually - seperated, thus the fracture surface energy G_{Ic} is of the order of the surface work parameter γ. With growing chain length entanglements are being formed which establish a physical network. At $T < T_g$ entanglements are stable. If, therefore, in the course of a fracture process a chain has to be seperated from such a network, this can only be done after considerable deformation of several chains, i.e. after a certain plastic deformation. Thus, fracture energy and generally strength and thoughness as well increase with the volume effected by the plastic deformation.

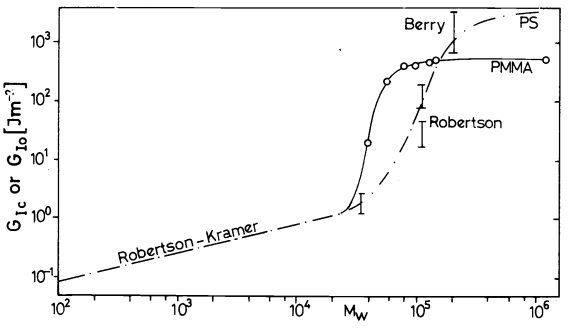

Fig. 1. Fracture surface energy (G_{Ic} or G_{Io}) vs molecular weight for PMMA (own measurements) and PS (literature values).

From these remarks it can be deduced that a plastic material will most likely be damaged if the **molecular chains are degraded or weakened,** if the **network is disentangled, plasticized or embrittled,** and if **local stress concentration** occurs through inclusions, flaws or internal tensions.

In the following a number of examples for each of these defects will be given.

STRENGTH EFFECTS OF MOLECULAR AND STRUCTURAL DEFECTS

Chain degradation

The principal consequences of production or service related chain degradation are the reduction of molecular weight, plasticization through monomer formation, and/or embrittlement through crosslinking reactions or chain weakening. There are several potential mechanisms for the destruction of long chain molecules as for instance **mechanical rupture** (2), **thermal decomposition** and **UV degradation.** A given polymer is generally not equally susceptible to all types of destruction since the mechanisms are different. The polysulfone (PSU) is an example in cause. Thus, it shows excellent mechanical strength and thermal resistance at temperatures up to and beyond 160 °C. If exposed to UV irradiation, however, it degrades fairly rapidly. In the latter process **main chain scission** occurs at the phenyl-C, phenyl-O and phenyl-S bonds (3), side group reactions involve the CH_3-groups. The formed free radicals react with oxygen leading to the appearance of new, oxygen containing groups such as -OH, -CHO or -COOH (Fig. 2). The molecular weight decreases notably during such an irradiation: from M_w 72 000 at t_{irr} = 0 to M_w = 19 000 at t_{irr} = 75 h. Concurrently the tensile strength and the extensibility of the irradiated film samples decrease (Fig. 3).

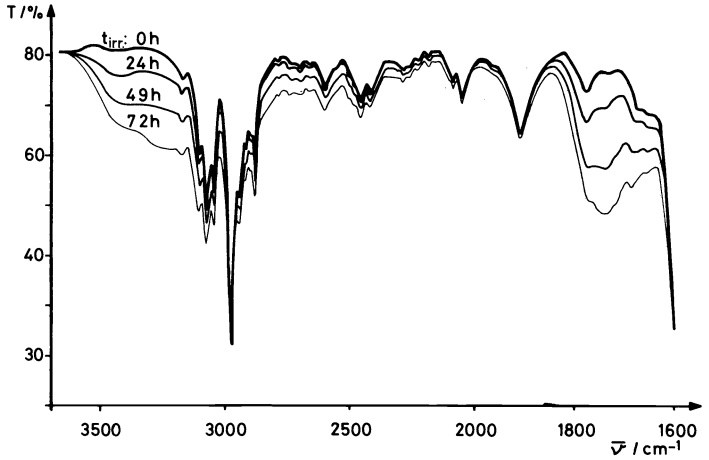

Fig. 2

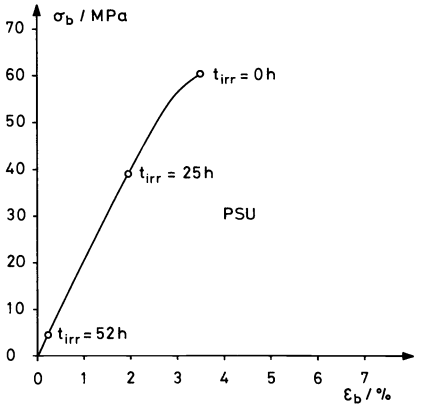

Fig. 3

Fig. 2. Part of the IR spectrum of UV irradiated polysulfone films of 17 µm thickness; t_{irr} indicates exposure time to accelerated aging in Xenotest 150; notable decreases of transmission in the region of O-H stretch and C=O stretch vibrations.

Fig. 3. Decrease of uniaxial strength σ_b of 17 µm thick polysulfone film strips exposed to accelerated aging in Xenotest 150 (o indicate point of rupture).

An almost opposite behavior is shown by polymethylmethacrylate (PMMA). Irradiation by UV does not measurably influence the molecular weight and the mechanical properties. However, it is well known that PMMA is susceptible to **depolymerization** at high temperatures ($T \geq 200\ ^0C$). The formed monomer may act as plasticizer and reduce yield and rupture stresses at temperatures just below T_g.

The influence of **thermal oxidation** on the mechanical behavior of polymers has been known for a long time. Understandably, processing is very often the most critical moment because of the necessarily higher extrusion or molding temperatures. If, for instance, the extrusion conditions of polyethylene pipes are not well controlled, layers of oxidized material are formed at the inside pipe surfaces (4-6). These layers, which are very brittle, have been studied in detail by Gedde, Jansson and Terselius (4-5). Two mechanisms contribute to an embrittlement of the material: the weakening of the backbone chain by formation of carbonyl groups and the crosslinking of neighboring chains by C-O-C bridges. The authors identified both types of bonds (-C=O; -C-O-C-) by IR reflectance spectroscopy at the inside walls of some HDPE pipes extruded at 200 ^0C. The thoroughly oxidized layers extended to a depth of some 20 to 160 μm. These layers were extremely brittle and cracked upon drawing at strains of a few per cent. The times to fracture in static loading of internally pressurized pipes (average hoop stress $\bar{\sigma}_t$ = 4.2 MPa, T = 80 ^0C) and of uniaxial creep samples, cut from the wall, were considerably shorter in the case of oxidized material. The final cracks seemed to originate at a distance of 0.2 to 0.3 mm from the oxidized layer (4).

On the basis of these investigations it may be suggested that one can distinguish in the oxidized HDPE pipes four different layers (distances s are with respect to the inner wall):

s = 0 - 100 μm thoroughly degraded, brittle material, $\sigma_t(s) = 0$
s = 150 - 250 μm somewhat degraded, readily creeping material, $\sigma_t(s)$ small
s = 300 - 500 μm slightly damaged zone, $\sigma_t(s) \sim \bar{\sigma}_t$
s > 500 μm normal material

The slightly damaged zone still contains numerous defects which favors creep craze initiation, and it also offers the required stress level. This combination results in a high probability for an early crack initiation in that zone. The cracks then propagate into the normal material. This mechanism explains well the observed shorter times to failure in oxidized pipes. In fact, Müller and Gaube report (6) that by carefully removing the oxidized layer the times to failure could be considerably improved and were equal to those of undamaged pipes.

The above explanation correlates also very well with an observation to be discussed later, namely that the time to fracture of LDPE pipes turns out to be shorter than the average lifetime whenever the final crack had started close to the inside or outside surface of the pipe wall (see further below).

Network defects

It has been pointed out in the introduction that solid polymers can be considered as **networks of chain segments interconnected by entanglements, crosslinking points and/or crystalline regions.** Whereas the elastic and anelastic properties are very often determined by the interaction of the individual segments, there is no doubt that the ultimate properties depend on the **network structure** (1-2).

The characteristic parameters of an amorphous network are evidently packing density, orientation distribution and correlation of chain segments, distribution of entanglement and crosslinking points and density of chain ends. These parameters fluctuate in space and time. Since each of them influences the mechanicsl response of a material, there will also be a **fluctuation of the local strength** of the network. This hypothesis is generally accepted. Nevertheless, there is a long and winding path between this hypothesis, and the statement that failure of a (or a few) volume elements will give rise to the breakdown of the whole structure.

Some of the characteristic parameters can conveniently be measured by light scattering. Studying polycarbonate (PC) Dettenmaier and Kausch (7) found modest **density fluctuations** with a correlation length of about 90 nm which were ascribed in part to holes, dust particles or additives. There was **no evidence for orientation correlation** between chain segments even after prolonged annealing below T_g. The annealing (150 h at 130 ^0C) did, however,

increase the yield stress by about 30 %. With respect to further details concerning methods, molecular models and relevance of conclusions, reference will be made to the comprehensive review article by Wendorff (8) on the structure of amorphous polymers.

In this section, particularly one parameter will be discussed which has turned out to be very important and which has attracted attention almost from the beginning of polymer science: the role of entanglements in the ultimate deformation of polymers. Douglas and Stoopes (9) as early as 1936, Flory (10), Haward (11), and many later researchers (12-14) have found a mostly linear relationship between uniaxial macroscopic strength, σ_b, of a network and $1/M_n$:

$$\sigma_b = \sigma_\infty(1-2\ M_e/M_n) \qquad (1)$$

with M_e being the average molecular weight of a chain segment between two adjacent entanglement points. This treatment is equivalent to considering the influence of molecular weight only through the "dangling chain ends" which do not contribute to the load carrying capability of the network. Important deviations from this relationship have been noted (13-14) at low and very high molecular weights. Drastically simplified theoretical calculations of σ_∞, based on Bueche's model of the ideal brittle strength of crosslinked rubbers (12) are, however, "within the ball park" (13-14). In these calculations it is assumed that the ideal strength of an isotropic entanglement network is given by the force nf_b it takes to break those (n) chain segments which intersect a unit area oriented perpendicularly to the stress axis:

$$\sigma_b = nf_b = \left(\frac{\rho N_A}{3M_e} \right)^{2/3} f_b \left(1 - \frac{2M_e}{M}\right). \qquad (2)$$

Whereas n and f_b have been quite correctly estimated, it has **completely been neglected that the chain segments in an isotropic polymer matrix have a statistically coiled conformation.** Thus, before being loaded by a force of the order of f_b a chain segment with end-to-end distance $\langle r_e^2\rangle^{1/2}$ would have to be stretched by a draw ratio

$$\lambda = (\langle r_e^2\rangle / L_s^2)^{1/2}, \qquad (3)$$

where L_s is the extended length of the segment. The thus defined values of λ range from about 2 to 5 for the most common amorphous polymers (15). This means that at least locally the network must deform heavily, possibly in an unstable manner. In order to predict reliably the ideal brittle strength of a polymer, it is therefore necessary to know the critical conditions for the onset of large deformations, to identify their limits (for instance in terms of the natural draw ratio λ_{nat}) and to ascertain the role of the entanglement network. Work to do just this has been going on in Lausanne for a number of years. Some results will briefly be presented here.

Entanglements and fracture

In a recent publication (16) Kausch and Dettenmaier have pointed out that the role of entanglements in glassy polymers evidently must be somewhat different from that in polymer melts and concentrated solutions. In particular the following aspects have to be taken into consideration:

- the lifetime and strength of an entanglement at a temperature below T_g must be considered to be very large;
- at small deformations (below craze initiation) hardly any molecular weight effects and consequently no entanglement effects become apparent;
- at larger deformations as for instance during crazing it is the presence of entanglements which permits the formation of stable fibrils; entanglement coupling is also the limiting factor in the orientational extension;
- the ultimate strain and energy of fracture strongly depend on the presence of entanglements; it is through this dependence that part of the calculations of the theoretical strength of an entanglement network, as mentioned before (11-14), gave not entirely unreasonable values.

Starting from the idea that the gradual disentanglement of molecules constitutes a major mechanism in the long time and fatigue failure of polymers (2,6) Kausch and Jud in 1978 began to develop a fracture mechanics method with which the mechanical effects of entanglement formation could be measured quantitatively. Experimental details (17-19) and results (1,17-21) of this method have been published elsewhere. It seems to be sufficient, therefore, to recall the principal observations.

Compact tension specimens as shown schematically in Figure 4 permit the determination of the fracture toughness K_{Io} by propagating a crack through the material (17-19). The formed crack will gradually heal at temperatures above T_g by interdiffusion of molecular coils across the interface. Thus, a certain fracture toughness K_{Ii} is reestablished in the fracture zone which can be determined in a second fracture experiment. Some results for PMMA 7 H are represented in Figure 5.

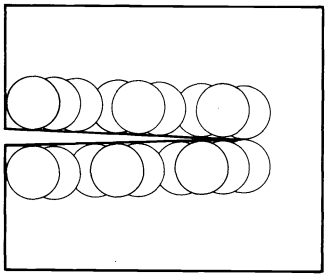

Fig. 4. Schematic representation of molecular coils at fracture surfaces before crack healing; the healing process is brought about by the reptational diffusion of molecules across the interface at $T > T_g$.

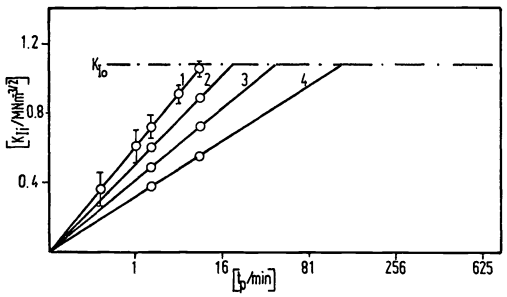

Fig. 5. Crack healing in PMMA 7 H: Fracture toughness vs $t_p^{1/4}$

1. T_p = 390 K 2. T_p = 385 K
3. T_p = 382 K 4. T_p = 378 K

These studies and also the recent experiments of Wool and collaborators (22) have clearly shown that there is a linear proportionality between the square of the fracture toughness K_{Ii} of the rehealed crack zone and the square root of the rehealing time t_p. It was quite possible to explain the observed time- and temperature-dependence of K_{Ii} by a diffusion model of chain interpenetration (18-22). Using additional IR experiments the Lausanne group also succeeded to determine the absolute value of the longitudinal diffusion coefficient of reptating chain molecules. For PMMA 7 H (M_w = 130 000) they obtained at 390 K a tube diffusion coefficient D_t of $32.5 \cdot 10^{-20}$ m^2/s. At t_p = 60 000 s this leads to a longitudinal distance travelled of 200 nm which corresponds roughly to the extended length of an average chain molecule (253 nm).

An analysis of the microscopic fracture process at the crack tip showed (19-20) that fracture proceeded through the formation and rupture of crazes (Fig. 6). The length s of the crazed zones observed at the crack tip increased linearly with the chain interpenetration previously achieved during

healing. The energy associated with the formation of the crazed zones corresponded very well to the fracture energy G_{Ii} of the rehealed samples which in PMMA amounted to 13 to 380 J m^{-2}, depending on the degree of healing. Based on the experience (24,25) that the simple pull out of non-entangled chains from a matrix requires fracture energies of 0.1 to 1 J m^{-2}, one can savely conclude that the interdiffusion of chains during rehealing must have involved the formation of entanglements (16).

Fig. 6. Interference micrograph of a crack front in partially healed PMMA 7 H (from 20).

The strong influence of entanglements on the fracture energy G_{Io} of virgin specimens is also revealed by the experimental data plotted in Figure 1. The fracture energy G_{Io} is related to the fracture toughness K_{Io} of the virgin material by:

$$G_{Io} = \frac{K_{Io}^2}{E(T,t)} (1-\nu^2) \qquad (4)$$

where E(T,t) is Young's modulus and ν Poisson's ratio. It is well observed that G_{Io} rises notably when the chains reach a length which is larger than that of the critical molecular weight M_c. Only at such a length the molecules can form a coherently entangled physical network.

As already stated before (16) two facts seem to be important with regard to the topology and number of entanglements in the interfacial region. First, it should be noted that according to the mode of entanglement formation through chain reptation **any new entanglement will necessarily be formed at the chain end** and then eventually be transferred along the chain. Thus, the stress transfer in the interfacial region of incompletely healed specimens must be assured by the newly formed entanglements of which a large proportion is sitting close to the end of the chain. The second fact concerns the initially more or less irregular local distribution of new entanglements within the former fracture surface. This variation diminishes with healing time. The less well healed zones with small craze bands undoubtedly constitute defects where crack growth occurs preferentially (Fig. 7).

Fig. 7. Slow crack growth in partially healed material; growth occurs preferentially in zones with smallest craze band (from 20).

These two facts should be borne in mind when one analyzes the mechanism of craze and fibril formation in incompletely healed specimens. In the interfacial region of such specimens there are fewer entanglements than elsewhere, and they are found close to the chain ends. It must then be assumed that in the process of fibrillation especially the newly entangled chains are highly stressed and **that they are gradually loosing those entanglements which are close to the chain ends.** Evidently the complete dissolution of the new entanglements in a particular cross-section of a fibril will lead to the rupture of that fibril. The above assumption would conveniently explain the observed correlation between the extent of fibril deformation and rehealing (19,20).

In conclusion it may be said that entanglements between molecules are necessary to stabilize the stress transfer between segments and prevent their rapid separation. In those plastics used for load bearing applications there will generally be more entanglements per molecule than needed to stabilize rapid stress transfer. Small local fluctuations of entanglement density, therefore, seem to be of no consequence. If, however, the number of entanglements per molecule is notably decreased then there will be volume elements with uncoupled molecules which constitute defect sites. A decrase of entanglement concentration can occur through chain scission, flow or long-time loading (2,6,16) or through fatigue loading (26).

Craze initiation

The formation of **intrinsic crazes** (crazes II) as recently observed by Dettenmaier and Kausch (27-30) clearly constitutes an instability which depends on the network properties and is not restricted to the sample surface. As opposed to this, **conventional or extrinsic crazes** are initiated in the neighborhood of flaws or dust particles and/or by traces of crazing agents preferentially at the specimen surfaces (Fig. 8).

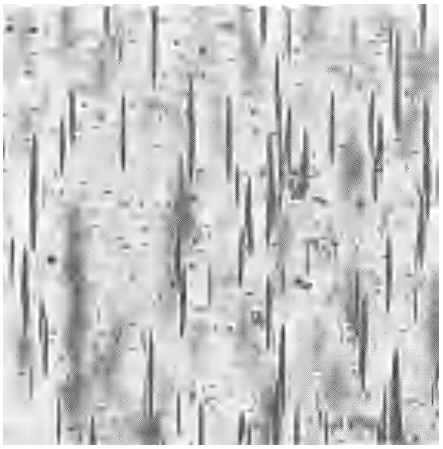

Fig. 8. Conventional crazes (crazes I) in preoriented polycarbonate subsequently stretched at 119 ^{0}C to ε = 42 %.

The initiation of the very large number (Figs. 9 and 10) of crazes II leads to an inflexion or a drop of the engineering stress-strain curve and, therefore, craze initiation may easily be identified. It has been demonstrated that crazes II are initiated in originally unoriented PC at an extension ratio of about λ^{II} = 2.1 (27). This value agrees rather well with the maximum extensibility of chains between entanglement points, λ^{nat}. Therefore, it must be assumed that disentanglement of chains either by chain slippage or by chain rupture plays an important role for craze II formation and growth.

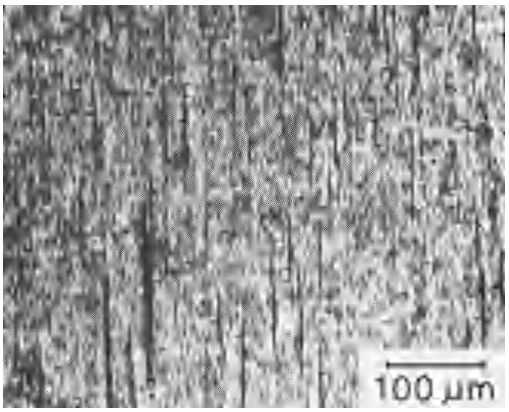

Fig. 9. Crazes I and intrinsic crazes (crazes II) in preoriented polycarbonate subsequently stretched at 119 ^{0}C to ε = 57 %.

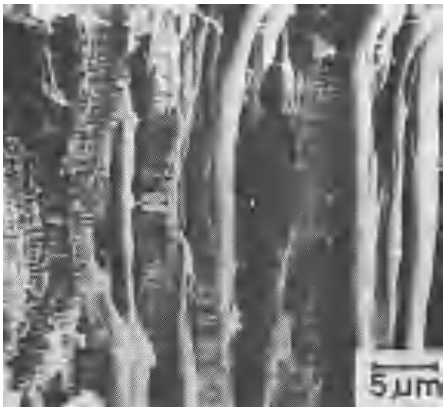

Fig. 10. Scanning electron micrograph of the fibrillar structure of crazes II in oriented polycarbonate.

Microstructure in crosslinked networks

Thoroughly crosslinked thermosetting resins have crosslink densities of about 0.1 to $2 \cdot 10^{21}$ cm^{-3}, i.e. average distances between crosslinks of 1 to 2 nm. A priori one has to expect, therefore, that fluctuations in the physical structure of the crosslink network will involve volume elements of a similar size. Evidently it is difficult to determine quantitatively structure variations in the nm-range. The current literature reflects this difficulty. There are reports on nodular regions of high crosslink density, 10 to 60 nm but also 6 000 to 10 000 nm in diameter, on small particles 6 to 9 nm in size which flow past each other during straining, and of optically discernable nodules 1 mm in diameter (31-33). The sizes of the so called intrinsic flaws, c, are calculated from strength σ, Young's modulus E and surface energy γ according to the Griffith equation:

$$c = 2 E\gamma / \pi\sigma^2 \qquad (5)$$

to be about 50 µm.

There is no unified view on the influence of these factual or hypothetical irregularities on the fracture behavior of cured resins. Mijovic et al. (31) state that the local plastic deformation and the critical energy release rate G_{Ic} are determined by internodular flow and are correlated with nodule size.

Mention should also be made of what may well be a special case. Morgan et al. (32) studied lightly amine-cured epoxy resins in the form of rather thin specimens. They observed in these glasses flow, crazing, shear banding

and cracking. They concluded that perfectly homogeneous crosslinked networks favored homogeneous plastic deformation whereas less perfect networks favored inhomogeneous deformation in the form of crazing and/or shear banding (33).

FLAWS AND INCLUSIONS

Almost any brittle fracture surface contains traces of a flaw or an inclusion which automatically will be blamed for having started the final crack and reduced the strength or time to failure of the specimen. Whereas the first point (origin) can generally be determined unambigously , the second is less clear, particularly if the flaws or inclusions originally are small.

This article can not attempt to review the abundant literature on stress concentration effects of cracks or particles and on the numerous electron microscopical investigations as to the origin of polymer failures. But a few remarks concerning the location of flaws and inclusions will be made.

In order to identify systematically the nature and position of defects in (LDPE) pipes Stockmayer and Wintergerst (34) developed a cutting technique which permitted to transform the entire pipe wall into a continous thin peeling of 0.06 to 0.15 mm thickness. By inspecting this film they were able to correlated nature, frequency and position of defects with time to failure t_b of the pipes. The irregularities they found were clear zones not mixed with carbon black in the form of points, linear marks, hooks (Fig. 11) and parallel striations. They claim that with a certain preference the final creep crazes originated in those areas of the pipe wall where the irregularities were more frequent. It was particularly noted by them that the lifetimes t_b of those pipes where the creep crazes had started close to the inner or outer surface of the pipe wall were an order of magnitude smaller ($\bar{t}_b$ = 740 h) than those where the crack had originated in the center ($\bar{t}_b$ = 7 400 h). Although the differences in stress distribution within the pipe wall, due to frozen-in tensions (see next section), may influence crack initiation it seems to be more probable that network defects are mostly responsible for this observation. As discussed in the preceeding section the inner walls of extruded pipes down to a depth of 0.5 mm are the first to experience an eventual network degradation. It was precisely in this region that Stockmayer and Wintergerst found the origins of the most rapid failures (34).

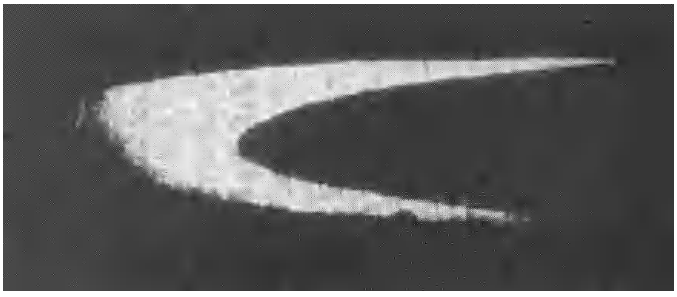

Fig. 11. Zone of about 3 mm length in an LDPE pipe which escaped mixing with carbon black (from Stockmayer, 34).

To test the influence of the observed irregularities further the authors performed tensile drawing and static loading experiments on samples cut from the peelings. In these experiments, there was practically **no correlation between yield stress and time to failure** on the one hand and **kind and concentration of flaws and inclusions** on the other. However, the effective elongation of films containing defects was much smaller since the necking samples generally broke whenever the neck had reached the defect. This behavior confirms the statements made before (2) and in the previous section, namely that creep craze nuclei must be considered as network defects which are not detectable in short time loading tests unless the defective zone is locally subjected to large deformations.

Evidently the question on the influence of inclusions added in the form of blending components or fillers is of vital importance to the fabrication and use of polymer composites. This problem has, therefore, been dealt with comprehensively under Topic IV of this meeting.

OTHER PRODUCTION RELATED DEFECTS

Geometry

A simple variation in sample cross-section can turn out to be a decisive defect. Thus, the **ductile failure** of uniaxially or biaxially loaded samples generally takes place at the smallest cross-section (Fig. 12). It should be noted that the failing section may be perfectly safe at higher stresses (brittle fracture) or longer times (creep crazing), because the breakdown in those cases is initiated by network defects or flaws.

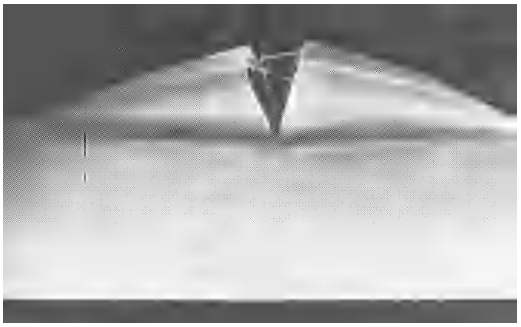

Fig. 12: Ductile failure of HDPE pipe (σ_v = 7 MPa, T = 80 °C, t_b = 0.5 h).

Internal tensions

Any viscoelastic body cooled from outside from above its solidification temperature (T_g or T_m) to a lower temperature T_c deforms non-homogeneously and either bends or contains frozen-in tensions. The distribution and absolute value of such tensions can be determined from a layer removal experiment (35). In pipes they generally show a parabolic distribution, compressive at the outside, smaller and tensile at the wall inside. Williams (35) derived the thermal, circumferential stresses $\sigma_R(s)$ as:

$$\sigma_R(s) = \frac{\alpha E(t')}{1-\nu} (T_m - T_c) \left(\frac{Nu}{2+Nu} \right) \left| \frac{1}{3} - \left(\frac{s}{W} \right)^2 \right| \qquad (6)$$

with:

s	distance from inside wall
α	coefficient of thermal expansion
E(t')	Young's modulus at time after cooling down
ν	Poisson's ratio
Nu	Nusselt number
W	wall thickness

For a HDPE pipe he had determined (compressive) stresses of -3 MPa at the outside and a tensile component of +1 MPa at the inside. Compared with the externally applied values of 15 to 20 MPa the frozen-in tensions are not entirely negligible.

Orientation distributions

Structure anisotropy is one of the characteristic properties of chain molecules and of any oriented polymer matrix. Many injection molded or extruded samples show signs of anisotropy (birefringence, extent of shrinkage). The HDPE pipe represented in Figure 12 gives an excellent example. The heavily deformed zone consists of molecules highly oriented in circumferential direction. In this direction fracture strength has considerably increased (perhaps by a factor of 10). Although the largest stress component still acts in this direction rupture occurs in axial direction, perpendicularly to the chain axis.Thus, a growing crack preferentially separates chains

instead of breaking them (the fibrils bridging the crack only underline this statement).

Weld lines

Welding, simple, rapid and straightforward, constitutes the most important technique for assembling thermoplastic construction elements. The final welds mostly distinguish themselves clearly from the main material by their form (upset, beads, camber, see Figs. 13 and 14), thermal history (and ensuing morphological changes), state of orientation and molecular interpenetration. Often less obvious are those weld lines created by the impingement of flowing masses in a mold or around the spider in an extrusion head. There again good molecular interpenetration is essential. This basic element of welding, the build-up of strength through entanglement formation, has been discussed in detail in an earlier section. At this point some experimental resuls on weld (line) strength will be added.

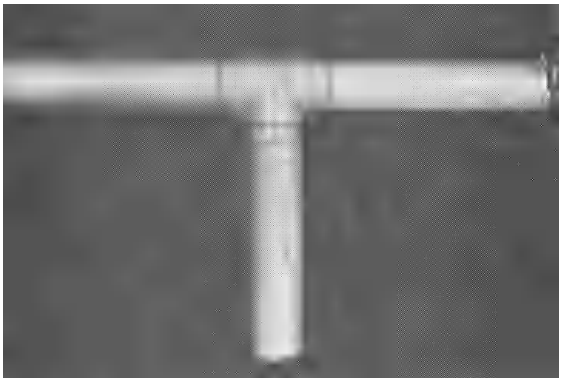

Fig. 13. Polypropylene T-joint butt-welded to three pipe sections; the T-joint was injection molded in two identical halves subsequently welded.

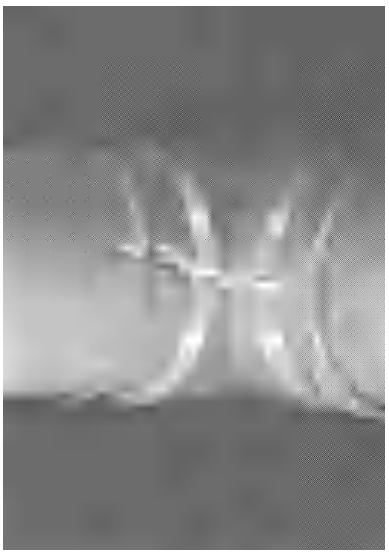

Fig. 14. Close up of left-hand corner of above specimen after test (7 bar, 95 ^{0}C); failure occurred within the weld plane of the T-joint itself, possibly in the very corner.

Crawford (36) has conceived a mold with typical features such as corners, changes in section, flow welds etc. and has carried out what he calls "pseudo-moldings". In his tests with PP the weld lines turned out to be the most notable defect.

Moslé et al. (37) molded PC plates with two central holes. By simply changing the stretching direction of these plates in subsequent tensile tests they could either load their specimens parallel (a) or perpendicular (b) to the weld lines. Their principal observation was that the yield **stresses** were more or less identical within a range of molding temperatures varying between 300 and 340 °C. The post-yield **strains,** however, were drastically smaller in case b. The rapid disintegration of the weld line material during plastic deformation is also underlined by the lower rupture forces (a/b = 2 200/1 100). Once again it has been demonstrated that strain hardening, a vital property for engineering thermoplastics, can only occur if the molecules are reliably interconnected so that they do not disentangle at the onset of plastic deformation.

Acknowledgement - The author would like to thank Drs. W. Müller and E. Gaube, Frankfurt/M.-Höchst, for having provided some of the test specimens and for valuable discussions.

REFERENCES

1. H.H. Kausch, IUPAC MACROMOLECULES, H. Benoit & P. Rempp Eds., Pergamon Press, Oxford-New York, 211 (1982).
2. H.H. Kausch, Polymer Fracture, Springer, Berlin-Heidelberg-New York (1978).
3. B. Rånby, J.F. Rabek, Photodegradation, Photo-oxidation and Photostabilization of Polymers, Wiley, London-New York (1975).
4. U.W. Gedde, On the necking and fracture behaviour of polyethylene, PhD Thesis, Royal Institute of Technology, Stockholm (1980).
5. U.W. Gedde, B. Terselius, H.-F. Jansson, Polymer Testing 2, 85 (1981)
6. W. Müller, E. Gaube, Kunststoffe 72, 297 (1982).
7. M. Dettenmaier, H.H. Kausch, Coll. & Polym. Sci. 259, 209 (1981).
8. J.H. Wendorff, Polymer 23, 543 (1982).
9. S.D. Douglas, W.N. Stoops, Ind. Eng. Chem. 28, 1152 (1936).
10. P.J. Flory, J. Am. Chem. Soc. 67, 2048 (1945).
11. R.N. Haward, The Strength of Plastics and Glass, Cleaver-Hume Press, London, Chap. II (1949).
12. F. Bueche, Rubber Chem. Tech. 32, 1269 (1959)
13. B.H. Bersted, J. Appl. Polym. Sci. 24, 37 (1979).
14. D.T. Turner, Polymer 23, 626 (1982).
15. E.J. Kramer, Lecture series on Polymer Micromechanics, Swiss Federal Institute of Technology, Department of Materials, Lausanne (1982).
16. H.H. Kausch, M. Dettenmaier, Coll. & Polym Sci. 260, 120 (1982).
17. K. Jud, H.H. Kausch, Polymer Bulletin 1, 697 (1979).
18. K. Jud, H.H. Kausch, J.G. Williams, J. Mater. Sci. 16, 204 (1981).
19. K. Jud, PhD Thesis 413, Swiss Federal Institute of Technology, Department of Materials, Lausanne (1981).
20. L. Könczöl, W. Döll, H.H. Kausch, K. Jud, Kunststoffe 72, 46 (1982).
21. T.Q. Nguyen, H.H. Kausch, K. Jud, M. Dettenmaier, Polymer 23, 1305 (1982).
22. R. Wool, J. Polym. Sci., Polym. Letters Ed. 20, 7 (1982).
23. H.H. Kausch, K. Jud, 5th Int. Conf. on Deformation, Yield and Fracture of Polymers, Cambridge, 29.3.-1.4.1982, p. 9.1.
Plastics & Rubber Processing & Appl. 2, 265 (1982).
24. E.J. Kramer, J. Mater. Sci. 14, 1381 (1978).
25. R.N. Haward, H.E. Daniels, L.R.G., Treloar, J. Polym. Sci., Polym. Phys. Ed. 16, 1169 (1978).
26. P.E. Bretz, R.W. Hertzberg, J.A. Manson, J. Appl. Polym. Sci. 27, 1707 (1982).
27. M. Dettenmaier, H.H. Kausch, Polymer 21, 1232 (1980).
28. H.H. Kausch, M. Dettenmaier, Polymer Bulletin 3, 565 (1980).
29. M. Dettenmaier, H.H. Kausch, Polymer Bulletin 3, 571 (1980).
30. M. Dettenmaier, H.H. Kausch, Coll. & Polym. Sci. 259, 937 (1981).
31. J. Mijovic, J.A. Kovtsky, Polymer 20, 1095 (1975).
32. R.J. Morgan, in: Developments in Reinforced Plastics-1, Chapter 7, G. Pritchard Ed., Applied Science Publishers, London (1980).
33. R.J. Morgan, E.T. Mones, W.J. Steele, Polymer 23, 295 (1982).
34. P. Stockmayer, S. Wintergerst, 3R international 20, 274 (1981).
35. J.G. Williams, Plastics & Rubber Processing & Appl. 1, 369 (1982).
36. R.J. Crawford, 5th Int. Conf. on Deformation, Yield and Fracture of Polymers, Cambridge, 29.3.-1.4.1982, p. 38.1.
37. H.G. Moslé, R.M. Criens, Kunststoffe 72, 222 (1982).